

# Sideward Locomotion Control of Biped Robots Based on Dynamics Morphing

Hiroshi Atsuta<sup>1</sup> and Tomomichi Sugihara<sup>2</sup>

**Abstract**—This paper presents a biped locomotion control to step sideways based on the framework of the dynamics morphing. Since the proposed controller does not require detailed referential motion trajectories, it enables a robot to walk sideways at arbitrary velocity given at random timing. Sideward locomotion is realized by alternating the velocity following control and the self-excited oscillating control accompanying with the exchange of the supporting foot. Techniques to automatically update the referential position of the center of mass and phase for the consistent footstep are also proposed.

## I. INTRODUCTION

Biped robots are potentially capable of locomoting on various terrains, particularly ill-conditioned environments such as a disaster site. Biped control itself is a mathematically difficult problem and has been tackled by many studies so far [1]–[6]. The most sophisticated approach is to plan a detailed referential trajectory in advance and to get the robot to track the trajectory which might be slightly modified based on the acquired information on-site with a stabilizer [7]–[10]. A benefit of this approach is that it can utilize powerful solvers for the boundary-value problem and the stabilizer can be designed rather simply. It has also been proposed as a successful scheme to embed the planner which runs at a short cycle into the overall feedback loop, so that it can cope with larger perturbations exerted during motions [11]–[14]. A paradox is that, if it is possible to plan a detailed referential trajectory beforehand, it means that sufficient information about the environment such as the ground profile is already known. It cannot be guaranteed in ill-conditioned fields where biped robots are the most demanded.

A trajectory-free biped control has also been of interest in the field of robotics, which is obviously more challenging than the trajectory-based control. Although many efforts have been made to achieve robust walking on uneven terrains [15]–[18], most of them assumed too much simplified robot bodies with point-contact feet and sagittally-constrained body, for instance. Moreover, they are not compatible with standing control, which is required for practical task-executions.

Sugihara [19]–[23] proposed a paradigm of *dynamics morphing*, in which each motion controller is designed as the entire structure of the dynamical system comprising the robot body and the controller, and motion transition is represented as a continuous or discontinuous morphing of

the controller. It enables a variety of motion in a consistent, robust and responsive way. Standing [19], stepping [21], emergent step-out [22] and longitudinal walk [23] have been realized so far. The goal of this work is to achieve the omnidirectional locomotion and enhance the robot mobility. This paper focuses on the sideward walk as a milestone.

Sideward locomotion has a complex nature from the viewpoint of the dynamical system that the robot cannot simply follow the commanded velocity, since it has to avoid the collision between the pair of legs. This constraint makes the control harder than that for longitudinal locomotion. Each foot should have different roles to accelerate and decelerate the robot, which has not been discussed in the previous literature. Three ideas to design a controller which embodies this dynamics are (i) alternating the self-excited oscillating control and the velocity-following control in accordance with the supporting condition, (ii) switching of the footstep control accompanying with the alternation of global control scheme, and (iii) foot lifting control which incorporates with the velocity-following control.

## II. BIPED CONTROL BASED ON DYNAMICS MORPHING

In this paper we consider a simplified model. The model is shown in Fig. 1, where the mass of the whole body of a robot is concentrated on the center of mass (COM). Let us assign  $x$ ,  $y$  and  $z$  axes along with the longitudinal, lateral and vertical directions, respectively, as shown in Fig. 1. For the sake of simplicity, we assume that the inertial torque about COM is small enough to be neglected and the height of COM  $z$  is constant. This simplification is plausible provided that the mass of the leg is sufficiently smaller than that of the body. Suppose that we denote the position of COM and the zero-moment point (ZMP) by  $\mathbf{p} = [x \ y \ z]^T$  and  $\mathbf{p}_Z = [x_Z \ y_Z \ z_Z]^T$ , respectively, we can get the following simplified equations of motion:

$$\ddot{x} = \omega^2(x - x_Z) \quad (1)$$

$$\ddot{y} = \omega^2(y - y_Z), \quad (2)$$

where  $\omega \equiv \sqrt{g/z}$  and  $g = 9.8[\text{m/s}^2]$  is the acceleration due to the gravity. This indicates that COM can be controlled through ZMP manipulation [24]. Note that ZMP  $\mathbf{p}_Z$  is constrained to lie within the supporting region  $\mathcal{S}$  as

$$\mathbf{p}_Z \in \mathcal{S}. \quad (3)$$

This constrain condition makes it difficult to realize the biped locomotion because the robot must achieve the ZMP manipulation within the supporting region  $\mathcal{S}$  and the discontinuous

<sup>1</sup>Hiroshi Atsuta is with Department of Adaptive Machine Systems, Graduate School of Engineering, Osaka University, Japan [hiroshi.atsuta@ams.eng.osaka-u.ac.jp](mailto:hiroshi.atsuta@ams.eng.osaka-u.ac.jp)

<sup>2</sup>Tomomichi Sugihara is with Department of Adaptive Machine Systems, Graduate School of Engineering, Osaka University, Japan [zhidao@ieee.org](mailto:zhidao@ieee.org)

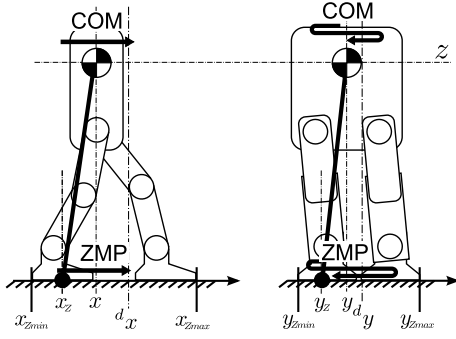


Fig. 1. An approximate mass-concentrated biped model

deformation of  $\mathcal{S}$  simultaneously. In particular, biped robots should carry out this operation with a pair of the right foot and the left foot.

Sugihara [23] has proposed the following biped control scheme which synthesizes the standing stabilization, the stationary alternate stepping and the longitudinal locomotion. The desired ZMP  $x_Z$  and  $y_Z$  treated as the control input of Eqs. (1) and (2) are defined as

$$\tilde{x}_Z = {}^d x + (q_x + 1) \left( x - {}^d x + \frac{\dot{x} - {}^d v_x}{\omega} \right) \quad (4)$$

$$x_Z = \begin{cases} x_{Zmax} & (\text{S1} : \tilde{x}_Z > x_{Zmax}) \\ \tilde{x}_Z & (\text{S2} : x_{Zmin} \leq \tilde{x}_Z \leq x_{Zmax}) \\ x_{Zmin} & (\text{S3} : \tilde{x}_Z < x_{Zmin}) \end{cases} \quad (5)$$

$$\tilde{y}_Z = {}^d y + (q_y + 1) \left( y - {}^d y + f(\zeta) \frac{\dot{y}}{\omega} \right) \quad (6)$$

$$y_Z = \begin{cases} y_{Zmax} & (\text{T1} : \tilde{y}_Z > y_{Zmax}) \\ \tilde{y}_Z & (\text{T2} : y_{Zmin} \leq \tilde{y}_Z \leq y_{Zmax}) \\ y_{Zmin} & (\text{T3} : \tilde{y}_Z < y_{Zmin}) \end{cases}, \quad (7)$$

where

$$f(\zeta) \equiv 1 - \rho \exp k \left\{ 1 - \frac{(q_y + 1)^2 \zeta^2}{r^2} \right\} \quad (8)$$

$$\zeta \equiv \sqrt{(y - {}^d y)^2 + \frac{\dot{y}^2}{\omega^2 q_y}}, \quad (9)$$

and  ${}^d x$  and  ${}^d y$  are the referential positions of COM,  ${}^d v_x$  is the referential velocity of COM along  $x$  axis,  $q_x (\geq 0)$ ,  $q_y (\geq 0)$ ,  $k (> 0)$ ,  $r (> 0)$  and  $\rho (\geq 0)$  are constant parameters to be designed. Here, the supporting region  $\mathcal{S}$  is simply represented by segments  $[x_{Zmin}, x_{Zmax}]$  and  $[y_{Zmin}, y_{Zmax}]$  along  $x$  and  $y$  axes, respectively. If the actual ZMP precisely tracks the desired ZMP, the motion of COM along  $x$  and  $y$  axes conform to the following piecewise autonomous systems:

$$\ddot{x} = \begin{cases} \omega^2 x - \omega^2 x_{Zmax} & (\text{S1}) \\ -\omega(q_x + 1)(\dot{x} - {}^d v_x) - \omega^2 q_x (x - {}^d x) & (\text{S2}) \\ \omega^2 x - \omega^2 x_{Zmin} & (\text{S3}) \end{cases} \quad (10)$$

$$\ddot{y} = \begin{cases} \omega^2 y - \omega^2 y_{Zmax} & (\text{T1}) \\ -\omega(q_y + 1)f(\zeta)\dot{y} - \omega^2 q_y (y - {}^d y) & (\text{T2}) \\ \omega^2 y - \omega^2 y_{Zmin} & (\text{T3}) \end{cases}. \quad (11)$$

Dynamical behaviors of the system governed by Eqs. (10) and (11) can be explained by means of phase portraits. First, let us consider the motion along  $x$  axis, namely the longitudinal direction. The control input in state (S2) i.e. Eq. (4) plays an important role in walking forward and backward and standing on site. Fig. 2(a) shows the phase portrait for the case of  ${}^d v_x = 0$  and  $q_x = 0.5$ . Other parameters are shown in the caption. Fig. 2(a) shows that COM state  $(x, \dot{x})$  stably converges to the reference. It means that this controller can be used as a standing stabilizer. In fact it coincides with the best COM-ZMP regulator [19]. On the other hand, substituting  $q_x = 0$  and nonzero value as  ${}^d v_x$  into Eq. (10), the following differential equation can be obtained,

$$\ddot{x} = -\omega(\dot{x} - {}^d v_x). \quad (12)$$

In this case the stationary point does not exist and  $\dot{x}$  converges to  ${}^d v_x$ . If  ${}^d v_x > 0$ , the state eventually goes into S1. If  ${}^d v_x < 0$ , it goes into S3. In whichever cases,  $\dot{x}$  will diverge. Fig. 2(b) is the phase portrait of the system for  ${}^d v_x = 0.2$  and  $q_x = 0$ . The transition between standing and walking is allowed by setting  ${}^d v_x$  and  $q_x$  to appropriate values. Besides the modulation of the controller, legged locomotion needs to involve footstep. In longitudinal direction, the midpoint of the feet can be a stable equilibrium point not only when standing on both feet as shown in Fig. 3(a) but also when standing on one foot as shown in Fig. 3(b). To prevent the divergence of  $\dot{x}$  and keep on moving, a control scheme of foot stepping which satisfies the standing stabilizability condition [19] all the time is proposed [23]. Fig. 4 shows that the robot behavior is continuously morphed between the standing stabilizer and the velocity following-control by setting  ${}^d v_x$  and  $q_x$ .

Next, let us consider the motion along  $y$  axis, namely the lateral direction. As shown in Eq. (6) the difference from the longitudinal controller is existence of the term  $f(\zeta)$ , which causes a nonlinear effect. Before handling the nonlinear term, let us consider the case that the nonlinear term is disappeared. Fig. 2(c) shows a phase portrait of the system for  $q_y = 0.5$  and  $\rho = 0$ . When  $\rho = 0$ , the nonlinear term in Eq. (6) is constant i.e.  $f(\zeta) = 1$  from Eq. (8) and this controller also coincides with the best COM-ZMP regulator in the same way as the longitudinal direction.

With the COM-ZMP regulator the robot can not step alternately because it is impossible to lift one foot with stabilizing COM asymptotically to the midpoint of the feet

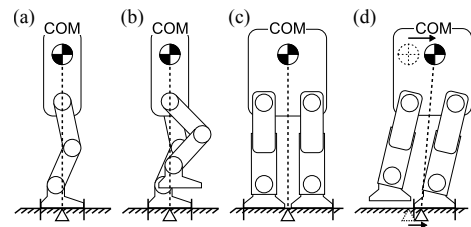


Fig. 3. Positions of equilibrium points

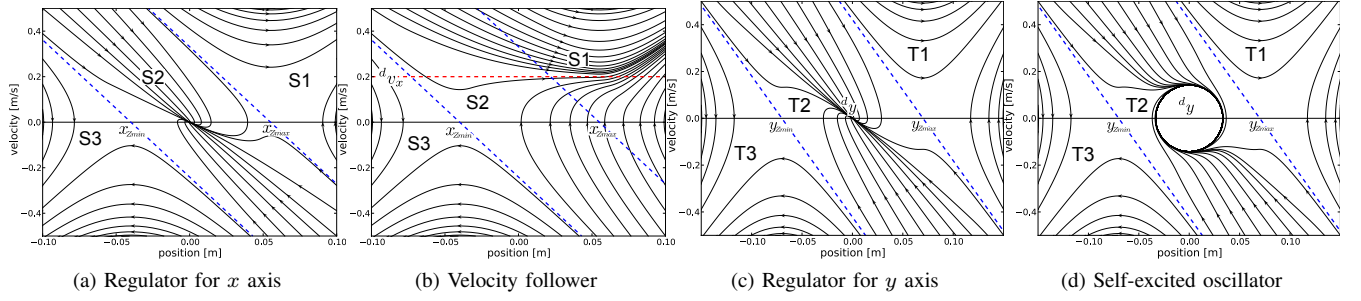


Fig. 2. Solution curves of the piecewise linear autonomous system for  $\omega = \sqrt{g/0.27}$ ,  $d_x = 0$ ,  $d_y = 0$ ,  $x_{Zmin} = -0.07$ ,  $x_{Zmax} = 0.07$ ,  $y_{Zmin} = -0.042$ ,  $y_{Zmax} = 0.042$ ,  $k = 1$  and  $r = 0.05$

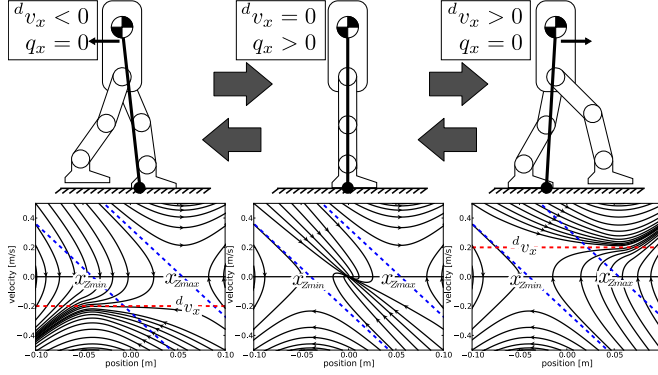


Fig. 4. Dynamics morphing along x axis

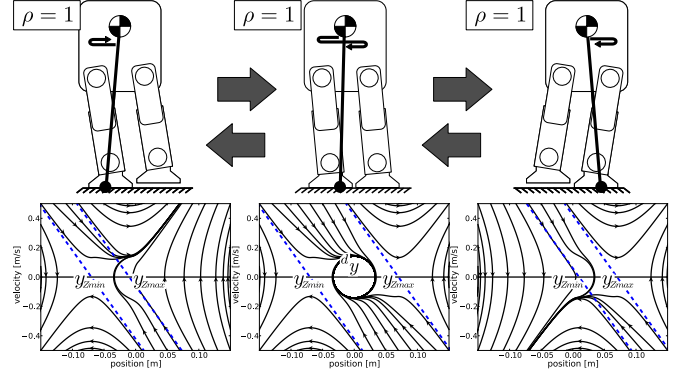


Fig. 5. Dynamics morphing along y axis

as shown in Fig. 3(c). Therefore, as shown in Fig. 3(d), COM needs to be located on the supporting foot so as to lift the other foot. Hence, to continue the stationary alternate stepping, it is needed to oscillate COM sideways. The nonlinear term  $f(\zeta)$  in Eq. (6) has the effect to arise the self-excited oscillation to COM. It emerges the following stable limit cycle in state (S2) when  $\rho > e^{-1}$ ,

$$(y - d_y)^2 + \frac{\dot{y}^2}{\omega^2 q_y} = \frac{(1 + \log \sqrt[4]{\rho}) r^2}{(q_y + 1)^2}. \quad (13)$$

In a particular case where  $\rho = 1$ , it represents a self-excited harmonic oscillator whose amplitude and period are  $\frac{r}{q_y + 1}$  and  $\frac{2\pi}{\omega \sqrt{q_y}}$ , respectively. Fig. 2(d) shows the phase portrait of the system for  $q_y = 0.5$  and  $\rho = 1$ . In the stationary state, the corresponding ZMP synchronizes the oscillation with the amplitude  $r$  without phase lag. Based on this fact, an alternate stepping control in which the dynamical constraint about ZMP is automatically satisfied has also been presented in [21]. Fig. 5 shows that in an alternate stepping the supporting region changes discontinuously and the phase portrait also changes.

### III. DYNAMICS MORPHING FOR SIDWARD LOCOMOTION CONTROL

#### A. Alternation of the velocity-following control and the self-excited oscillation control based on the supporting foot

Eqs. (1) and (2) are symmetric with respect to  $x$  and  $y$ . However, the controller for the longitudinal locomotion

described in the previous section can not be applied for the sideward locomotion. This is because in the longitudinal direction the robot can step in the direction of the referential velocity at any time, but in the sideward direction the robot can not always step in the direction of the referential velocity unless it is permitted the crossing of both legs. Let us think about the case in which the robot moves in the leftward. When the left foot is lifted off the ground, the robot can move leftwards by switching the controller to the velocity follower; when the left foot is landed on the ground, the robot will fail to move if the controller still remains in the velocity follower. Therefore, when the left foot is landed on the ground, it is needed to be switched to the self-excited oscillator to decelerate COM. To realize such a control scheme the lateral direction controller is replaced with the following instead of Eq. (6),

$$\ddot{y}_Z = d_y + (q_y + 1) \left( y - d_y + f(\zeta) \frac{\dot{y} - d_{v_y}}{\omega} \right), \quad (14)$$

where  $f(\zeta)$  is defined by Eq. (8) and  $d_{v_y}$  represents the referential velocity along  $y$  axis. This controller features coexistence of the self-excited oscillator with the velocity follower; it turns into the velocity follower which has the same structure as Eq. (4) when  $\rho = 0$  and  $q_y = 0$ , and it turns into the self-excited oscillator which coincides with Eq. (6) when  $d_{v_y} = 0$  and  $\rho = 1$ . According to the moving direction and the supporting condition, appropriate parameters should be set.

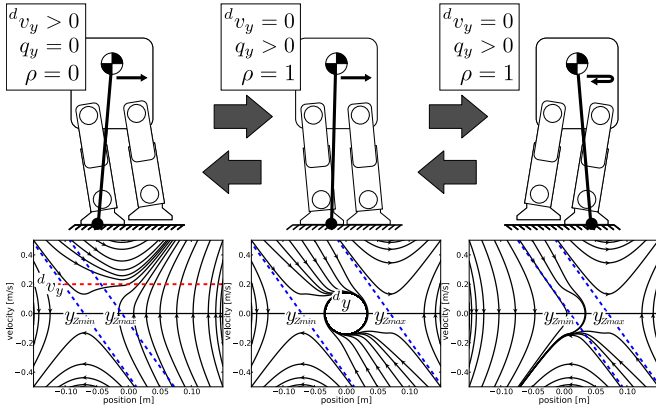


Fig. 6. Dynamics morphing along  $y$  axis with a desired velocity

Fig. 6 shows that the controller is automatically alternated between the velocity follower and the self-excited oscillator based on the state of the supporting foot.

### B. Automatic update of referential position

In the velocity following control, the referential positions of COM  ${}^d x$  and  ${}^d y$  disappear from the system and the robot moves independently of  ${}^d x$  and  ${}^d y$ . Thus, it is dangerous at the moment when the robot goes back to the standing stabilization to leave  ${}^d x$  and  ${}^d y$  intact during walking. While the longitudinal walking, updating the referential position of COM by the current position during  ${}^d v_x \neq 0$ , namely,  ${}^d x = x$  avoids such an unsafe situation as proposed in [23], in the sideward walking that is unsuccessful because the referential position  ${}^d y$  is the oscillation center of COM. In order to make the robot stop immediately or continue the alternate stepping on site, let us update the referential position of COM in the following way: only if the plus or minus of the velocity of COM  $\dot{y}$  matches with that of the referential velocity  ${}^d v_y$ , the referential position along  $y$  axis is updated by

$${}^d y = y + \text{sgn}(\dot{y}) \frac{r}{q_y + 1}, \quad (15)$$

where the second term of the right-hand side of Eq. (15) represents the oscillation amplitude of COM.

### C. Consistent footstep control with velocity follower

In the velocity following control, a consistent footstep control is needed for the avoidance of the divergence of COM. As proposed in [23], in the longitudinal direction it is successful in walking continuously to determine the desired landing position  ${}^d x_S$  of the swinging foot based on the standing stabilizability condition [19], namely,

$${}^d x_S = x + \frac{\dot{x}}{\omega}. \quad (16)$$

In the lateral direction, however, the same way is unsuccessful since COM oscillation causes an oscillation of the desired landing position defined by Eq. (16). So let us redefine the desired landing position of the swinging foot along  $y$  axis so that the referential position of COM  ${}^d y$  is located at the midpoint of the feet, namely,

$${}^d y_K = 2 {}^d y - y_P, \quad (17)$$

where  $K$  and  $P$  are for  $L$  and  $R$ , respectively, when the left foot works as the swinging foot, and for  $R$  and  $L$ , respectively, vice versa.

It should be needed to modulate the amplitude of the self-excited oscillation  $r$  as the width between the feet varies during the sideward locomotion, that is,

$$r = \frac{y_L - y_R}{2}. \quad (18)$$

### D. Consistent foot lifting control with velocity follower

In order to continue the locomotion, the up-and-down movements of the feet has to be synchronized with ZMP and the supporting region has to be intentionally deformed. It requires to abstract the phase information from the movements of COM and ZMP, the latter of which relates the phase with the supporting region. The following complex number  $p_Z$  is available for circularity-free definition of the phase:

$$p_Z \equiv y_Z - {}^d y - \frac{(\bar{q}_y + 1)(\dot{y} - {}^d v_y)}{\omega \sqrt{\bar{q}_y}} i \quad (19)$$

$$z_* \equiv \frac{1}{2} \frac{h|p_Z|}{r} \sigma(\bar{\rho})(1 - \cos 2\pi \phi_*), \quad (20)$$

where  $*$  means  $L$  or  $R$ .  $\phi_L$  and  $\phi_R$  are the lifting phases of each foot which is defined from the relative position estimated successively when  $p_Z$  is within the region of the supporting foot on the complex plane. See the literature [21] for the details.  $h$  is a constant parameter, meaning the maximum lifting height, and  $\sigma(\bar{\rho})$  is defined as follows:

$$\sigma(\bar{\rho}) \equiv \begin{cases} 1 & (\bar{\rho} > 1) \\ \bar{\rho} - e^{-1} & (e^{-1} \leq \bar{\rho} \leq 1) \\ 1 - e^{-1} & (0 \leq \bar{\rho} < e^{-1}) \\ 0 & (0 \leq \bar{\rho} < e^{-1}) \end{cases}. \quad (21)$$

$\bar{q}_y$  and  $\bar{\rho}$  are defined respectively, as follows:

$$\bar{q}_y \equiv \begin{cases} q_y & (q_y \neq 0) \\ q'_y & (q_y = 0) \end{cases}, \quad \bar{\rho} \equiv \begin{cases} \rho & (\rho \neq 0) \\ \rho' & (\rho = 0) \end{cases}. \quad (22)$$

As mentioned in Subsection III-A, in the case of switching the controller into the velocity follower by giving nonzero referential velocity, it is needed to set  $q_y = 0$  and  $\rho = 0$ , but this operation is inconsistent with Eqs. (19) and (21). In order to be consistent even in that case,  $q'_y$  and  $\rho'$  are set to the reserved values of  $q_y$  and  $\rho$  just right before being switched to the velocity following control.

## IV. SIMULATION

A simulation of a sideward locomotion is conducted based on the proposed controller. An anthropomorphic robot “mighty” [25] was supposed. In the robot model, the total mass was concentrated at COM for simplicity. The whole body motion is generated by solving inverse kinematics from COM and feet positions. The height of COM was  $z = 0.26[\text{m}]$ ,  $q_x = 0.5$ ,  $k = 1$  and  $h = 0.02[\text{m}]$ . The sideward stance width between the both feet was initialized to be  $0.1[\text{m}]$  ( $r = 0.05[\text{m}]$ ). Each foot is represented by a rectangle with the forward length  $0.055[\text{m}]$ , the backward length  $0.04[\text{m}]$ , the innerward length  $0.035[\text{m}]$  and the outward

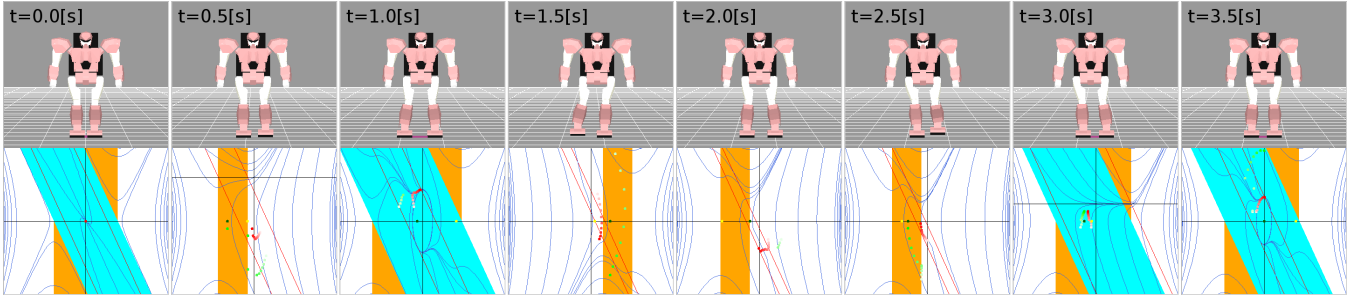


Fig. 7. Snapshots of the simulated sideward locomotion. The robot succeeded to continue walking with respect to  ${}^d v_y$  changed at random during the motion.

length 0.035[m]. While each foot turned to the swinging foot, a second-order lag controller to track smoothly the desired landing foot position defined by Eqs. (16) and (17) were validated as

$$\ddot{x}_* = K({}^d x_S - x_*) - C\dot{x}_* \quad (23)$$

$$\ddot{y}_* = K({}^d y_K - y_*) - C\dot{y}_*, \quad (24)$$

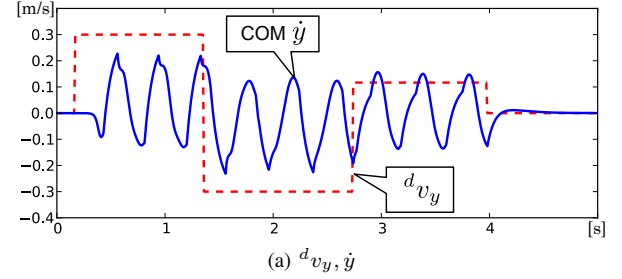
where  $*$  is for  $L$  or  $R$ ,  $x_L$  and  $x_R$  mean the positions along  $x$  axis of the left and right foot, respectively, and  $y_L$  and  $y_R$  mean the same way as  $x$  axis.  $K = 3000$  and  $C = 50$  were adopted in the simulation. The saturation rules in Eqs. (5) and (7) are substituted for the nearest point of the desired ZMP position on the supporting region. The differential equations were numerically solved by fourth-order Runge-Kutta's method with the quantized interval 0.01[s].

We developed a simulator to test the validity of the proposed controller. Some control parameters are forced to change without relation to given command parameters. Therefore, the set of command parameters was held separately from the set of control parameters so that the controller was able to reflect the command parameters as the control parameters at an appropriate timing.

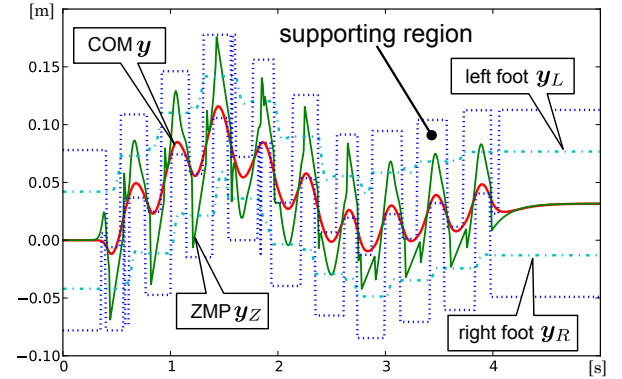
The initial condition was set for  $(x, \dot{x}, y, \dot{y}) = (0.0409, 0, 0, 0)$ ,  $q_y = 0.5$  and  $\rho = 0$ . During the simulation  ${}^d v_y$  was modified within the range of  $-3.0 \sim 3.0$ [m/s] at random, except for the last phase of the simulation in which  ${}^d v_y$  was set for 0[m/s] so as to return to the standing stabilization. Fig. 7 shows snapshots of the movie of the simulation. The history of the referential velocity of COM and the actual velocity of COM axis are plotted in Fig. 8(a), and the position of COM, the position of ZMP, the positions of feet and the supporting region are plotted in Fig. 8(b).

In spite of changing the command value  ${}^d v_y$  completely at random as shown in Fig. 8(a), Fig. 8(b) shows that the robot continues to walk sideways without falling with the manipulation of ZMP, the deformation of the supporting region and consistent foot steps, and the transition of starting, turnings and stopping was successfully achieved.

As we can see in Fig. 8(a), there are some moments when the derivative of the velocity of COM  $\dot{y}$  changes abruptly. Occurrence of these points in time is attributed to the alternation of the two controllers, i.e. the velocity-following control and the self-excited oscillation control. While in the velocity-following control  $\dot{y}$  approaches asymptotically to the



(a)  ${}^d v_y, \dot{y}$



(b)  $y, y_Z, y_L, y_R$

Fig. 8. Results of the simulation

referential velocity  ${}^d v_y$ , in the self-excited following control COM state converges to the limit cycle expressed in Eq. (13), which is independent of  ${}^d v_y$ . Fig. 9 shows trajectories of COM state in the phase space when  ${}^d v_y = 0.25$ [m/s] and  ${}^d v_y = 0.12$ [m/s] are given. As shown in Fig. 9(a), when  ${}^d v_y$  is large compared to the limit cycle,  $\dot{y}$  is drawn into the limit cycle by switching to the self-excited oscillator before  $\dot{y}$  reaches  ${}^d v_y$ . On the other hand, as shown in Fig. 9(b), when  ${}^d v_y$  is small compared to the limit cycle,  $\dot{y}$  exceeds  ${}^d v_y$  in the same way.

From Fig. 8(b) we can observe that there are sharp bending points in the trajectory of ZMP. This also results from the alternation of the two controllers. This phenomenon is not considered to be a problem for the present. One of the reasons of for this is that the motion of the robot is smooth enough as can be seen in the history of  $\dot{y}$  in Fig. 8(b). Another reason is that the discontinuous ZMP manipulation seems to be required for a rapid movement.

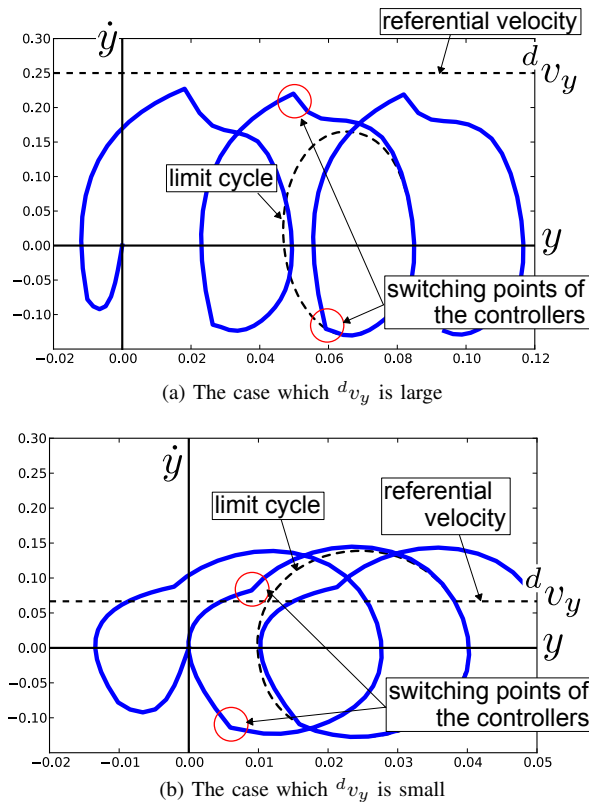


Fig. 9. Loci of COM in sideway locomotion

## V. CONCLUSION

A novel biped controller which realize the transition from the standing stabilizer to the sideward locomotion without planning time-dependent trajectories was developed based on the dynamics morphing. Realizing sideward locomotions require a suitable cooperation of acceleration and deceleration of COM. This is achieved by switching the velocity-following controller and the self-excited oscillation controller whether the supporting foot in the direction of the referential velocity is landing on the ground or not. This controller enables a robot to move consistently even when the referential velocity is given completely at random. A diagonal walking is also possible by giving the longitudinal referential velocity as well as the sideward referential velocity. A remaining issue is to expand it to an omnidirectional walking including rotation.

## REFERENCES

- [1] M. Vukobratovic, A. Frank, and D. Juricic, "On the stability of biped locomotion," *IEEE Transactions on Bio-Medical Electronics Engineering*, vol. BME-17, no. 1, pp. 25–36, 1970.
- [2] A. Takanishi, Y. Egusa, M. Tochizawa, T. Takeya, and I. Kato, "Realization of Dynamic Walking Stabilized with Trunk Motion," in *ROMANSY 7*, 1988, pp. 68–79.
- [3] K. Hirai, M. Hirose, Y. Haikawa, and T. Takenaka, "The development of Honda humanoid robot," in *Proceedings of the 1998 IEEE International Conference on Robotics and Automation*, vol. 2, 1998, pp. 1321–1326.
- [4] K. Loffler, M. Gienger, and F. Pfeiffer, "Sensor and control design of a dynamically stable biped robot," in *Proceedings of the 2003 IEEE International Conference on Robotics & Automation*, vol. 1, 2003, pp. 484–490.

- [5] K. Nagasaka, Y. Kuroki, S. Suzuki, Y. Itoh, and J. Yamaguchi, "Integrated motion control for walking, jumping and running on a small bipedal entertainment robot," in *Proceedings of the 2004 IEEE Conference on Robotics and Automation*, vol. 4, 2004, pp. 3189–3194.
- [6] T. Sugihara and Y. Nakamura, "Boundary Condition Relaxation Method for Stepwise Pedipulation Planning of Biped Robots," *Robotics, IEEE Transactions on*, vol. 25, no. 3, pp. 658–669, 2009.
- [7] F. Gubina, H. Hemami, and R. B. McGhee, "On the dynamic stability of biped locomotion," *IEEE Transactions on Bio-Medical Engineering*, vol. BME-21, no. 2, pp. 102–108, 1974.
- [8] R. Katoh and M. Mori, "Control method of biped locomotion giving asymptotic stability of trajectory," *Automatica*, vol. 20, no. 4, pp. 405–414, 1984.
- [9] T. Mita, T. Yamaguchi, T. Kashiwase, and T. Kawase, "Realization of a high speed biped using modern control theory," *International Journal of Control*, vol. 40, no. 1, pp. 107–119, 1984.
- [10] J. Pratt and G. Pratt, "Intuitive control of a planar bipedal walking robot," in *Proceedings of the 1998 IEEE International Conference on Robotics and Automation*, vol. 3, 1998, pp. 2014–2021.
- [11] J. Chestnutt, M. Lau, G. Cheung, J. Kuffner, J. Hodgins, and T. Kanade, "Footstep planning for the honda asimo humanoid," in *Proceedings of the 2005 IEEE International Conference on Robotics and Automation*, 2005, pp. 629–634.
- [12] S. Kajita, M. Morisawa, K. Harada, K. Kaneko, F. Kanehiro, K. Fujiwara, and H. Hirukawa, "Biped Walking Pattern Generator allowing Auxiliary ZMP Control," in *Proceedings of the 2006 IEEE International Conference on Intelligent Robots and Systems*, 2006, pp. 2993–2999.
- [13] K. Nishiwaki and S. Kagami, "Online Walking Control System for Humanoids with Short Cycle Pattern Generation," *International Journal of Robotics Research*, vol. 28, no. 6, pp. 729–742, 2009.
- [14] A. Herdt, N. Perrin, and P. B. Wieber, "Walking without thinking about it," in *Proceedings of the 2010 IEEE/RSJ International Conference on Intelligent Robots and Systems*, 2010, pp. 190–195.
- [15] S. Miyakoshi, G. Taga, Y. Kuniyoshi, and A. Nagakubo, "Three Dimensional Bipedal StepStep Motion using Neural Ooscillator - Towards Humanoid Motion in the Real World," in *Proceedings of the 1998 IEEE/RSJ International Conference on Intelligent Robots and Systems*, 1998, pp. 84–89.
- [16] M. Yamakita, F. Asano, and K. Furuta, "Passive velocity field control of biped walking robot," in *Proceedings of the 2000 IEEE International Conference on Robotics and Automation*, vol. 3, 2000, pp. 3057–3062.
- [17] S.-H. Hyon and T. Emura, "Symmetric Walking Control: Invariance and Global Stability," in *Proceedings of the 2005 IEEE International Conference on Robotics & Automation*, 2005, pp. 1455–1462.
- [18] C. Chevallereau, J. Grizzle, and C.-L. Shih, "Asymptotically Stable Walking of a Five-Link Underactuated 3-D Bipedal Robot," *IEEE Transactions on Robotics*, vol. 25, no. 1, pp. 37–50, 2009.
- [19] T. Sugihara, "Standing stabilizability and stepping maneuver in planar bipedalism based on the best COM-ZMP regulator," in *Proceedings of the 2009 IEEE International Conference on Robotics & Automation*, 2009, pp. 1966–1971.
- [20] —, "Dynamics morphing from regulator to oscillator on bipedal control," in *Proceedings of the 2009 IEEE/RSJ International Conference on Intelligent Robots and Systems*, 2009, pp. 2940–2945.
- [21] —, "Consistent biped step control with COM-ZMP oscillation based on successive phase estimation in dynamics morphing," in *Proceedings of the 2010 IEEE International Conference on Robotics & Automation*, 2010, pp. 4224–4229.
- [22] —, "Reflexive Step-out Control Superposed on Standing Stabilization of Biped Robots," in *Proceedings of the 2012 IEEE-RAS International Conference on Humanoid Robots*, 2012, pp. 741–746.
- [23] —, "Biped control to follow arbitrary referential longitudinal velocity based on dynamics morphing," in *Proceedings of the 2012 IEEE/RSJ International Conference on Intelligent Robots and Systems*, 2012, pp. 1892–1897.
- [24] K. Mitobe, G. Capi, and Y. Nasu, "Control of walking robots based on manipulation of the zero moment point," *Robotica*, vol. 18, pp. 651–657, 2000.
- [25] T. Sugihara, K. Yamamoto, and Y. Nakamura, "Hardware design of high performance miniature anthropomorphic robots," *Robotics and Autonomous Systems*, vol. 56, no. 1, pp. 82 – 94, 2008.